Energy Conversion and Management 80 (2014) 39–45

Contents lists available at ScienceDirect

Energy Conversion and Management

journal homepage: www.elsevier.com/locate/enconman

The step-change cooling performance of miniature thermoelectric module for pulse laser

Limei Shen [a], Huanxin Chen [a,*], Fu Xiao [b], Yaxin Yang [a], Shengwei Wang [b]

[a] Department of Refrigeration & Cryogenics, Huazhong University of Science and Technology, Wuhan, China
[b] Department of Building Services Engineering, The Hong Kong Polytechnic University, Kowloon, Hong Kong

ARTICLE INFO

Article history:
Received 19 September 2013
Accepted 2 January 2014
Available online 5 February 2014

Keywords:
Miniature thermoelectric module
Thermal resistance of hot-end heat exchanger
Scaling effect
Supercooling effect
Step-change

ABSTRACT

This article investigates a miniature thermoelectric module (MTEM) for pulse laser cooling. A step-changed cooling model is developed to predict the thermal performance of the MTEM. Interfacial effects of the MTEM are analyzed by considering the thermal non-equilibrium between electrons and phonons adjacent to thermoelectric/metal interface. Parametric studies were performed to analyze the effect of the pulse-width of laser, thermal resistance of hot-end heat exchanger, cooling load and the step-changed voltage on the system cooling performance. Particular attention is paid to the influence of scaling effect and supercooling effect on enhancing the miniature thermoelectric cooling (MTEC) performance. At a specific cooling load, the effects of pulse-changed and step-changed voltage on MTEC are numerically and experimentally studied. The MTEM can deal with not only the low cooling load of continuous laser, but also high cooling load of pulse laser which surpasses its' maximum cooling capacity. The transient response of cold-end temperature experiences an underdamped oscillation and finally reaching a steady-state value. A curve fitting equation for cold-end temperature is used to provide more accurate temperature and understand the temperature control strategy for pulse laser. The numerical result shows that the prediction by the model agrees well with the performance curve of datasheet and experimental data. It is also found that the voltage for achieving the maximum cooling capacity experiences step decrease with the increase of thermal resistance of hot-end heat exchanger.

1. Introduction

Laser is the high thermal flux electro-optic equipment where performance and reliability are a strong function of operating temperature. Research results indicate that a laser's wavelength–temperature sensitivity is about 0.2–0.5 nm/°C [1]. So, thermal management of semiconductor laser requires high heat flux cooling capability (>100 W/cm^2), tight temperature control (approx. ±2 °C), reliable start-up (on demand) and long term stability. Spray cooling, micro-channel, water chiller system, and thermoelectric cooling system are all used to cool the laser equipment, respectively. However, there is a technology challenge associated with the implementation and practice in the zero-gravity environment of spray cooling, micro-channel and water chiller system.

Thermoelectric cooler (TEC) is a promising solid-state active heat pump with high cooling power density and small feature size for micro-electronically integrated cooling [2,3]. The heat produced by electronic devices can be absorbed rapidly by TEC and dissipated through the radiator. They are widely employed in microelectronics to stabilize the temperature of laser diodes, to cool infrared detectors and charge-coupled devices, and to reduce unwanted noise of integrated circuits. But the conventional bulk TECs are incompatible with microelectronic fabrication process for laser cooling [3], the micro TECs are incompatible with little temperature difference and little cooling capacity for laser cooling [4]. Therefore, the miniature thermoelectric cooler (MTEC), is defined here as those whose maximum dimension is on order of millimeter (O(mm)), with a maximum dimension not to exceed about 1 cm, have been designed by using micromachining technology and can be integrated into microelectronic circuits for global cooling. Laser diodes traditionally have used MTECs for precision temperature control to improve diode output levels and maintain wavelength integrity [5,6]. It also demonstrated that if no TEC adopted in butterfly laser module, the power emitting from laser module will be reduced to 46% when ambient temperature rise from 20 °C to 85 °C [1].

To address the thermal problem of lasers, many investigators have researched interrelated thermal characteristics of semiconductor laser. In the actual laser diode operation, several modeling works of laser diode containing a TEM have been reported, by assuming the cold-side of TEM is kept at 25 °C for different ambient temperature [6–8]. Finite element models (FEMs) were all constructed using Ansys [7–12] or COMSOL [13] software. Their

* Corresponding author. Tel.: +86 189 7114 2396.
E-mail address: chenhuanxin@tsinghua.org.cn (H. Chen).

0196-8904/$ - see front matter © 2014 Elsevier Ltd. All rights reserved.
http://dx.doi.org/10.1016/j.enconman.2014.01.003

Nomenclature

A	cross-sectional area (m^2)
C	heat capacity ($J\,kg^{-1}\,K^{-1}$)
COP	coefficient of performance of thermoelectric cooling system
R_h	thermal resistance of hot-end heat exchanger ($°C\,W^{-1}$)
K	thermal conductivity ($W\,m^{-1}\,K^{-1}$)
L_{te}	length of thermoelectric element (m)
Q_c	heating load of laser (W)
t	time (s)
t_{pl}	the pulse width of laser (s)
t_{pu}	the holding time of the step-changed voltage U_p (s)
T	temperature (°C)
ΔT	the temperature difference between hot-end and cold-end of MTEM (°C)
I	electric current (A)
U	applied voltage (V)
U_p	the step-change voltage (V)
U_{Tcmin}	the voltage for achieving the minimum steady cold-end temperature T_{cmin} (V)
$U_{\Delta Tmax}$	the voltage for achieving the largest temperature difference between the hot-end and the cold-end (V)
x	coordinate (m)

Greek letters

α	seebeck coefficient of thermoelectric module ($V\,K^{-1}$)
α_{pn}	seebeck coefficient of thermoelectric element ($V\,K^{-1}$)
ρ	density of thermoelectric elements ($kg\,m^{-3}$)
σ	electrical conductivities ($\Omega^{-1}\,m^{-1}$)

Subscripts

c	cold-end of the TE element
h	hot-end of the TE element
a	ambient

investigations showed that main factors that affect the TEC performance are the heat generation of laser diode, thermal resistance of thermal path, heat exchanger, and the ambient temperature. Labudovic and Jin [5] built a three-dimensional finite element model of laser containing on thermoelectric cooling in ANSYS. The modeling results show good agreement with the experimental results obtained by IR thermometry. Novak et al. [14] compared a standard pulse-width modulation controller and a variable-voltage controller based on TEMs for a thermal management system of pulse laser. They showed that the design of the thermal management system based on the variable-voltage controller offers a significant performance advantage over the pulse-width modulation design. We realize that, for actual applications, it is important to discuss the transient characteristics of MTEM for laser to enhance the cooling performance.

According to the above review of previous research on thermal management of laser with TEC, it observed that previous studies mainly focused on investigation of the thermal characteristics of laser in a FEM software, by assuming the cold-side temperature of TEM is a constant. However, there is no open report on the analytical model to study the performance of MTEM for laser diodes. Actually, the cooling capacity of MTEM is little for laser, especially for pulse laser with high thermal flux. So it is important to enhance the performance of MTEM by introducing the transient supercooling effect. Furthermore, the cold-side temperature of MTEM is a function of time, especially for the pulse laser with pulse cooling load. So it is important to study the transient characteristics of MTEM for laser cooling. However, the performance of the TEM is much sensitive to the thermal resistance between the TEM and the ambient air [2,15]. In addition, the operating ambient temperature variation range of laser is from −20 °C to 70 °C [13]. But the previous study generally assumed the ambient temperature is 25 °C. So it is important to discuss the influence of thermal resistance between the MTEM and the ambient to maintain the temperature of laser under higher ambient temperature.

2. Description of the mathematic model

A SP5083 is used to study the performance of typical MTEM [16]. The performance specifications of SP5083 are listed in Table 1 in this work [17]. The dimension of MTEM is smaller than bulk TEM, but larger than micro TEM. The thickness L_{te} of thermoelectric leg of SP5053 is about 1 mm, so whether the interfacial effects will affect the thermal distribution of thermoelectric element should be discussed.

The phonon and electron thermal and electrical boundary resistances are different, respectively. So the Joule heating and Peltier cooling/heating are also different adjacent to the interface, which will require a distance (δ), so-called as cooling length, to reach equilibrium [18,19]. The cooling length of SP5083 is 0.15645 μm. The electron and phonon temperature distribution along the thermoelectric element are computed according to the literature [18]. We observed that L_{te} = 0.2222 mm is the critical value for considering the interfacial effects. So the simulation model of bulk TEM is suited for the MTEM.

The transient cold-end temperature (T_c) of MTEM is the most important monitoring value for laser thermal management. So a one-dimensional partial differential Eq. (1) is proposed to obtain the T_c. Firstly, the heat load of laser (Q_c) is considered as a constant. Secondly, at t = 0 s the whole element has the uniform initial temperature T, which equals the ambient temperature (T_a).

The thermal partial differential equation of thermoelectric element [15,20]:

$$\rho C\frac{\partial T}{\partial t}=k\frac{\partial^2 T}{\partial x^2}+\frac{I^2}{\sigma A^2} \tag{1}$$

Initial conditions:

$$T(:,0)=T_a \tag{2}$$

Boundary conditions:

$$x=0,\ \rho A\frac{dx}{2}C\frac{dT_c}{dt}=Q_c+kA\frac{\partial T}{\partial x}|_{x=0}+\frac{I^2dx}{2\sigma A}-0.5\alpha_{pn}IT_c \tag{3}$$

$$x=L,\ \rho A\frac{dx}{2}C\frac{dT_h}{dt}=0.5\alpha_{pn}IT_h+\frac{I^2dx}{2\sigma A}+kA\frac{\partial T}{\partial x}|_{x=L}-(T_h-T_a)/R_h \tag{4}$$

The energy conversion of thermoelectric leg is described by Fig. 1 [21,22]. The equations are derived using the finite volume method according to the law of energy conservation along the length direction of the TE leg. The following assumptions are made in solving the differential equation. Firstly, the length of the finite

Table 1
Parameters of SP5083.

Type	Couples N	Current I_{max} (A)	Voltage U_{max} (V)	Maximum cooling capacity Q_{max} (W)	Maximum temperature difference between hot-end and cold-end $\triangle T_{max}$ (°C)	Reference temperature at hot-end T_h (°C)	Dimensions
SP5083	23	1.9 1.8	2.61 3.31	3.2 4.0	65 86	27 85	6.02(L) × 8.18(W) × 1.65(H)

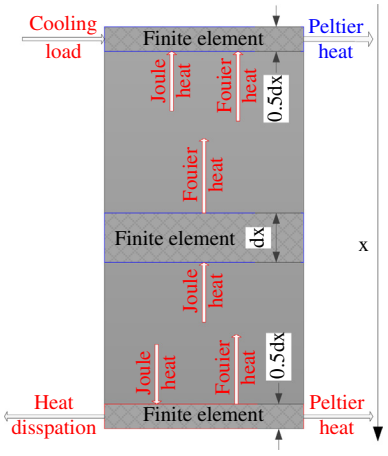

Fig. 1. Energy conversion of thermoelectric leg.

element is set for '*dx*'. Secondly, the length of the finite element is set for '*dx*/2' to extract the temperature values of the cold-end and hot-end. For Eq. (1), the left hand represents that the thermal increase rate of finite element. The right hand represents the Fouier heat and Joule heat of the finite element. For Eq. (3), the left hand represents that the thermal increase rate of finite element at the cold-end. The right hand represents the Fouier heat, Joule heat and Peltier cooling. For Eq. (4), the left hand represents that the thermal increase rate of finite element at the hot-end. The right hand represents the Fouier heat, Joule heat and Peltier heating. Joule heat is the volume heat generation. Fouier heat is thermal conduction which is proportional to the magnitude of the temperature gradient and opposite to it in sign. Peltier cooling absorbed heat at the cold-end, and Peltier heating release heat at the hot-end.

The total voltage across the terminals of a TEM is composed of the voltage generated by Seebeck effect and the voltage drop due to the module's internal electrical resistance. Where I in equations can substitute with the following equation:

$$I = (U - \alpha(T_h - T_c))/R \quad (5)$$

Here, The MTEM Seebeck coefficient α, the MTEM internal electrical resistance R and the MTEM thermal conductance K are 0.0092 V K^{-1}, 1.3973 Ω, 0.0263 W m^{-1}K^{-1}, respectively [23,24]. The Seebeck coefficient α_{pn}, the thermal conductivity k, the electrical conductivity σ of the thermoelectric leg are 0.0004 V K^{-1}, 1.7791 W m^{-1} K^{-1} and 105776 Ω^{-1} m^{-1}, respectively [15,20]. The volumetric heat capacity thermoelectric element C is 200 J kg^{-1} K^{-1}, the density of thermoelectric element ρ is 10922.08 kg m^{-3} [15,25].

3. Numerical simulation results and discussion

Generally, the laser works in a large range of ambient temperature (−20 °C to 70 °C) [13]. The requirement for the operating temperature of the lasers is becoming more demanding; the module has to work with good stability within a wide range of case temperatures (T_c) between 0 °C and 75 °C [5]. But, most applications will maintain at a constant temperature (typically 25 °C). For ambient temperature >25 °C, MTEM can absorb heat from the laser by taking in direct electrical voltage. For ambient temperatures <25 °C, MTEM can pump heat to the laser by taking in a reverse voltage. The laser device is usually operating integrated with other electric components, so the operating ambient temperature is usually higher than conventional ambient temperature. To predict the cooling performance of MTEM under high ambient temperature, the ambient temperature (T_a) is set for 70 °C.

Thermal resistance (R_h) is a very important parameter as it is the bottleneck for effective heat removal from the hot end of the TEM to the ambient, which can increase the temperature at the cold junction of TEC and laser, especially in high temperature environment.

3.1. The steady-state cooling performance of MTEM at lower and higher ambient temperature

The hot-end heat exchanger of the TEM, which is used to release the hot-end heat generation of TEM to the environment, has an important influence on cooling performance of TEM. So it's not feasible to choose MTEMs for laser cooling according to the datasheet. The relationship between the performance and thermal resistance of heat exchanger is studied for selecting a TEM that thermally "matches" the heat exchanger used in practical application. To explore the practical maximum cooling capacity of SP5083 when the cold-end temperature maintains at 25 °C, the range of the thermal resistances of hot-end heat exchanger considered in this paper is assumed to be 0–10 °C W^{-1}. The steady-state cooling performance is studied to examine the practical maximum cooling capacity of SP5083.

The voltage U_{Qcmax} for achieving the maximum cooling capacity Q_{cmax} of SP5083 at different R_h is shown in Fig. 2. The Q_{cmax} decreases with the increase of R_h. The maximum cooling capacity of

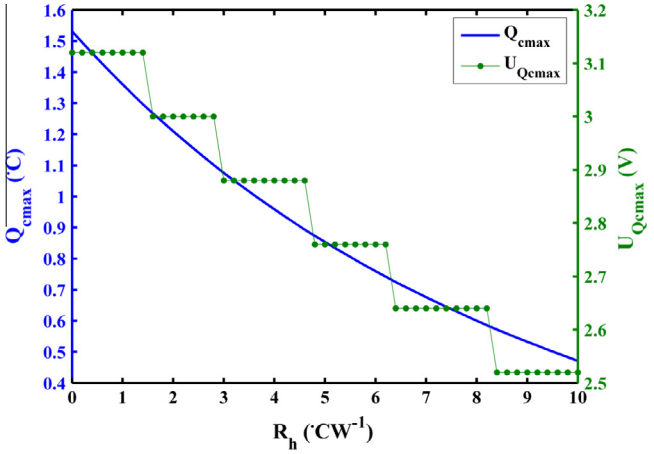

Fig. 2. The voltage U_{Qcmax} for achieving the maximum cooling capacity Q_{cmax} to ensure the cold-end temperature maintain at 25 °C when T_a = 70 °C.

SP5083 is 1.53 W when R_h is equal to 0 °C W^{-1}, and the voltage U_{Qcmax} for achieving the maximum cooling capacity Q_{cmax} is 3.12 V.

There is an interesting phenomenon for U_{Qcmax}. Fig. 2 shows the U_{Qcmax} experiences step decrease with the increase of R_h. It is because the response of the cooling capacity is the result of the combined action of the Peltier cooling, Fourier heat and Joule heat. The cold-end temperature maintains at constant value. When R_h is small, the heat at the hot-end is released to the ambient in time, the hot-end temperature and Fourier heat slowly increases with the increase of R_h. The Peltier cooling decreases with the increase of temperature difference. The Joule heat decreases because the Seebeck voltage offsets part of the applied voltage. However, the decrease of Peltier cooling offsets the decrease of Joule heat and the increase of Fourier heat. Therefore, the U_{Qcmax} maintains at constant at first. Then, as the increase of R_h, the heat at the hot-end cannot be released to the ambient in time and reversely transfers to the cold-end which adversely increase the hot-end temperature and Fourier heat. It breaks the above thermal equilibrium. It must decrease the applied voltage U_{Qcmax} to decrease the Joule heat, which is the dominated heat source according to Eq. (3). Then, in the next region, U_{Qcmax} maintains at constant again. So U_{Qcmax} experiences step decrease with the increase of R_h.

The resistance of hot-side heat exchanger for TEC is reviewed. For micro-channel, the range of resistance is 0.5–4 °C W^{-1} [25], the resistance of a flat micro-heat pipe (The maximum heat transport per unit area is 1.3 × 10^5 W/m^2) is 1 °C W^{-1} [26,27]. According to the above analysis, the thermal resistances R_h in this paper is set for 2 °C W^{-1}. The cooling load is set for 1 W and 10 W.

Assuming Q_c = 0 W, the steady-state cold-end temperature (T_c) and temperature difference (ΔT) profile at different ambient temperature is shown in Fig. 3. It shows that T_c decreases with the increase of U at first and reaches its minimum value, then increases with the increase of U. This is because that the Peliter cooling is proportional to the voltage and the Joule heating is proportional to the square of voltage and opposite to it in sign. The cold-end temperatures for the same applied voltage at the steady-state in Fig. 3 are different. It can be attributed to different hot-end heat exchanger and ambient temperature. The vary of ΔT is opposite to the vary of T_c. When R_h = 0 °C W^{-1} and T_a = 85 °C, the voltage for achieving the minimum cold-end temperature and the voltage for achieving the maximum temperature difference are both equal to 3.36 V, respectively. The maximum temperature difference is equal to 86 °C. The values are consistent with the datum of Table 1. When R_h = 2 °C W^{-1} and T_a = 70 °C, the voltage for achieving the minimum cold-end temperature is 3 V, and the voltage for achieving the maximum temperature difference is 3.48 V.

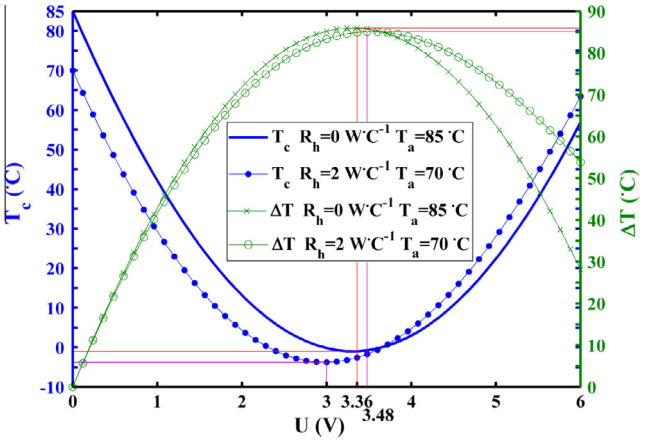

Fig. 3. The steady-state cold-end temperature (T_c) and temperature difference ΔT under different R_h when Q_c = 0 W.

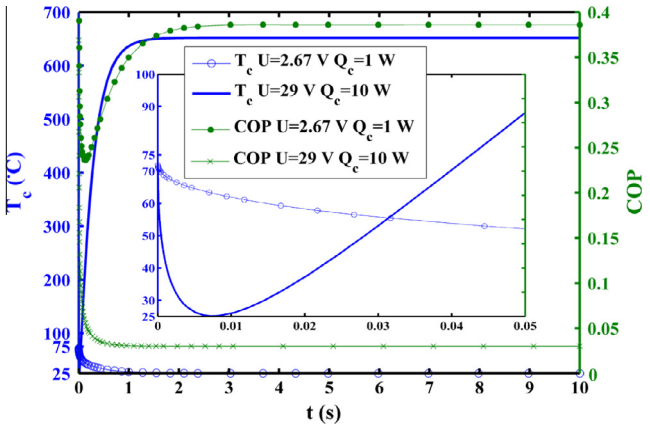

Fig. 4. The transient varies of cold-end temperature (T_c) and COP$_c$ under different Q_c when R_h = 2 W °C^{-1}.

3.2. The transient-state cooling performance

The transient cold-end temperature and coefficient of performance (COP) are analyzed at different cooling load are applied to SP5083, as shown in Fig. 4. It shows that when the cooling load of laser is 1 W, the cold-end temperature decreases with time at first and then maintains at 25 °C. The COP decrease to 0.23 at first, and then increase with time and finally maintains at 0.385. But when cooling load of laser is 10 W, the cold-end temperature decreases to 25 °C with time at first, then increases with time and finally maintains at 652 °C. The COP decrease with time and maintains at 0.003. This is because that the cold-end temperature is the result of the combined action of the cooling load, Peltier heat, Fourier heat and Joule heat. The Peltier heat dominates at the cold-end in the very beginning. Then, the influence of the cooling load and Joule heat become larger than others, when the cooling load or applied voltage is larger. Therefore, the cold-end temperature is too large when cooling load is equal to 10 W and the applied voltage is equal to 29 V, respectively.

The above analysis illustrates that the MTEM will lose cooling capacity when cooling load is larger than 1.53 W. So the transient supercooling effect of TEC is introduced for the pulse laser with high thermal flux [15,28], which can obtain an instantaneously lower temperature than that reachable at steady-state.

3.3. The pulse supercooling for pulse laser

To investigate the transient supercooling effect for pulse laser with high thermal flux, the step changes were introduced into the applied voltage. The cooling load pulse in a period as a function of time is given by

$$Q_c = \begin{cases} 0, 0 \leqslant t < 5 \\ 10, 5 \leqslant t < 5 + t_p \\ 0, 5 + t_p \leqslant t < 10 \end{cases} \quad (6)$$

where t_p is the pulse-width of laser. When the cooling load is 0 W and the applied voltage U is 1.662 V, the cold-end temperature is maintained at 25 °C. So the applied voltage pulse in a period as a function of time is given by

$$U = \begin{cases} 1.662, 0 \leqslant t < 5 \\ U_p, 5 \leqslant t < 5 + t_p \\ 1.662, 5 + t_p \leqslant t < 10 \end{cases} \quad (7)$$

where U_p is the applied voltage pulse of MTEM. Shen et al. [15] demonstrated that when the applied voltage suddenly changes from U to U_p, the voltage pulse will produce a large transient supercooling temperature if $U_p > U$, it will produce an overshoot in the cold-end temperature if $U_p < U$. However, it is of crucial importance to maintain the laser diode temperature in a narrow range during operation in order to achieve satisfactory performance and reliability of the laser. Therefore, a proper U_p is repeatedly calculated and analyzed to ensure the temperature accuracy (±2 °C). To analyze the influence of pulse-width, the t_p is set for 0.01 s, 0.02 s, 0.05 s and 0.1 s, respectively. The applied voltages change to 8 V at 5 s, and then change back to 1.662 V at $(5 + t_p)$ s. To analyze the influence of U_p, U_p is set for 8 V and 10 V. The comparison is carried out when the t_p is 0.05 s and 0.1 s, respectively.

Fig. 5 shows that the transient responses of cold-end temperature when a cooling load pulse and a voltage pulse are applied. When the applied voltage suddenly changes from 1.662 V to U_p at 5 s, the cold-temperature drops immediately and then slowly increases with time. There is an overshoot for cold-end temperature when the applied voltage suddenly changes from U_p to 1.662 V at $(5 + t_p)$ s. The overshoot increases with the increase of t_p and U_p, respectively. It is because the response of the cold-end temperature is the result of the combined action of the Peltier heat, Fourier heat, Joule heat and cooling load. The overshoot illustrates that the transient supercooling effect of MTEM enhances the Peltier heat and puts off the effect of cooling load. And the overshoot is much larger than 2 °C.

Comparing Fig. 4 with Fig. 5, it may be feasible to utilize step-changes voltage to reduce the time to reach the stable temperature and decrease the overshoot. The parameters of pulse-width of laser and the step-changes of applied voltage are repeatedly calculated and analyzed to develop a similar second-order underdamped profile for cold-end temperature.

The cooling load in a period is given by Eq. (8)

$$Q_c = \begin{cases} 0, 0 \leqslant t < 4 \\ 10, 4 \leqslant t < 4.02 \\ 0, 4.02 \leqslant t < 10 \end{cases} \tag{8}$$

But the applied voltage in a period experiences step change from 1.662 V to 8 V at 4 s, change to 2.8 V at 4.02 s, change to 2.15 V at 4.05 s, change to 1.84 V at 4.25 s, then change to 1.7 V at 4.55 s, and finally change back to 1.662 V at 5.05 s. The pulse cooling load, the input step voltage U and the response of

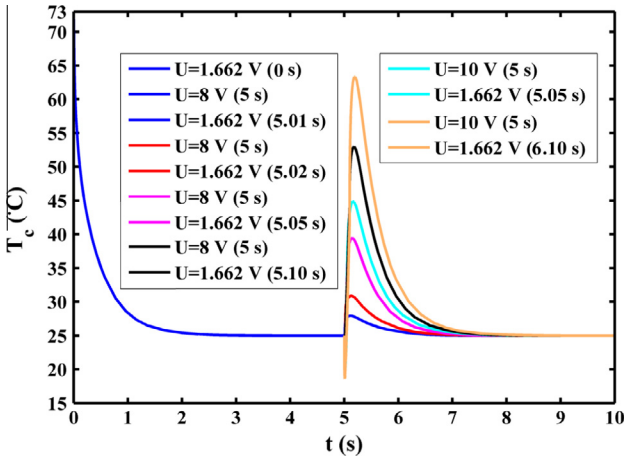

Fig. 5. The transient responses of cold-end temperature (T_c) when a cooling load pulse and a voltage pulse are applied.

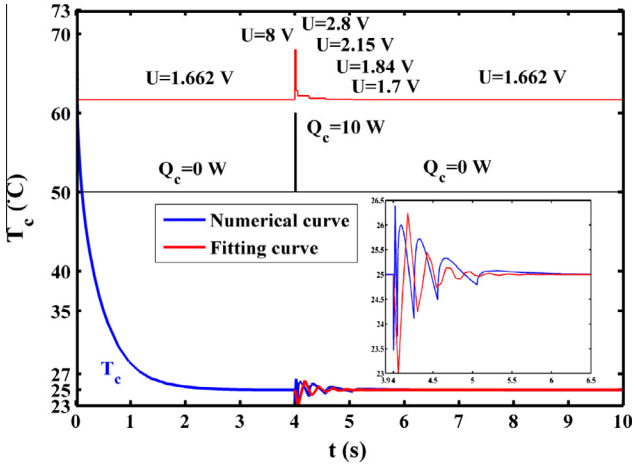

Fig. 6. The transient responses of cold-end temperature (T_c) when a cooling load pulse and a step-changed voltage are applied.

cold-end temperature profile with blue line are as shown in Fig. 6, where the red line in the plot represents the fitting curve. The response of cold-end temperature is similar to the underdamped oscillation. It shows that the cold-end temperature maintains at 25 ± 2 °C. Comparing Fig. 5 with Fig. 6, the transient supercooling effect can reduce the applied voltage to achieve the required temperature.

A series of calculations was carried out to construct parameters for the fitting equation. The equation of cold-end temperature is fitted according to second-order underdamped step function. The fitting equation of T_c is given by

$$T_c = 25\left(1 - 0.1e^{-\varepsilon\omega_n(t-4)}\sin(\omega_n\sqrt{(1-\varepsilon^2)}(t-4))\Big/\sqrt{(1-\varepsilon^2)}\right) \tag{9}$$

where ε is equal to 0.15, ω_n is equal to 25. It helps to understand the action of controller design and to provide a control strategy for the temperature controller of pulse laser.

4. Experimental study

A MTEC-based thermal management system of a pump laser system was set up. The experimental testing rig is shown schematically in Fig. 7. In measuring the transient response of cold-end temperature of SP5083, the pump lasers' heat-generating capability was mimicked using a set of 1 Ω elements, the element is placed in a copper shell, there is a convex platform structure to connect with the cold-end of SP5083. The hot-end of SP5083 was connected with a forced convection heat-sink. The thermal resistance of heat-sink is a function of operating temperature, so the transient response is shown in the following figures. The average value of R is 1.8 °C W^{-1} which is approximately equal to the setting numerical value. The DC voltage is supplied by KXN-6020D, the range of output DC voltage is −60 V to 60 V and the range of output DC current is −20 A to 20 A. The cold-end temperatures measured by type T thermocouples are transmitted to the data logger Keithley2700 and then to the computer via RS232 interface for analysis. The experimental equipment was housed in 70 °C thermostat.

The step-response simulations and the corresponding measurements were carried out in order to demonstrate the proposed step-change strategy of applied voltage for pulse laser as well as to compare the performance of pulse voltage and step-change voltage. With the heater turning on and off and the applied voltage of MTEM,

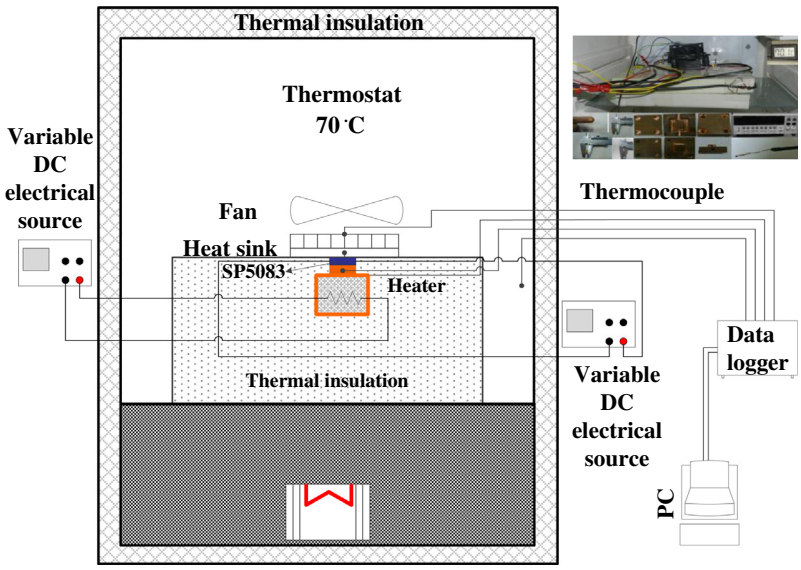

Fig. 7. The schematic diagram of experiment.

the resulting cold-end temperature of MTEM will be response to the changes of the applied voltage.

Two groups of experiment tests were performed. In the first group of tests, the applied voltages experienced one pulse change from 1.7 V to 8 V when the MTEM worked at the steady-state with applied voltage 1.7 V and sustained 30 s, then returned to 1.7 V. The cooling load experienced one pulse change from 0 W to 10 W and sustained 30 s, then returned to 0 W. The cold-end temperature, applied voltage and ambient temperature are shown in Fig. 8. In the second group of tests, the applied voltages experienced fifth step-changes, from 1.7 V to 8 V, 5 V, 3.3 V, and then to 2.5 V when the TEM worked at the steady-state with applied voltage 1.7 V, then returned to 1.7 V until the cold-end temperature reaches stable. The cooling load experienced one pulse change from 0 W to 10 W and sustained 30 s, then returned to 0 W. The cold-end temperature, applied voltage and ambient temperature are shown in Fig. 9.

Fig. 8 shows that a fixed voltage, i.e. 1.7 V, is supplied to MTEM at the beginning. The cold-end temperature of MTEM decreases rapidly, then the decreasing level becomes small, till T_c reaches stable at 41.9 °C. As the steady-state is achieved, the applied voltage and heater then starts pulse-change to 8 V and 10 W, respectively. T_c drops rapidly and reaches the minimum 41.7 °C,

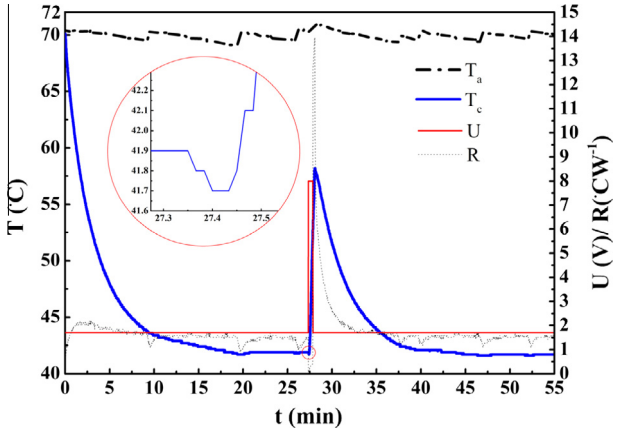

Fig. 8. Transient cold-end temperature (T_c) profiles of MTEM when cooling load and applied voltage respectively experienced one step change.

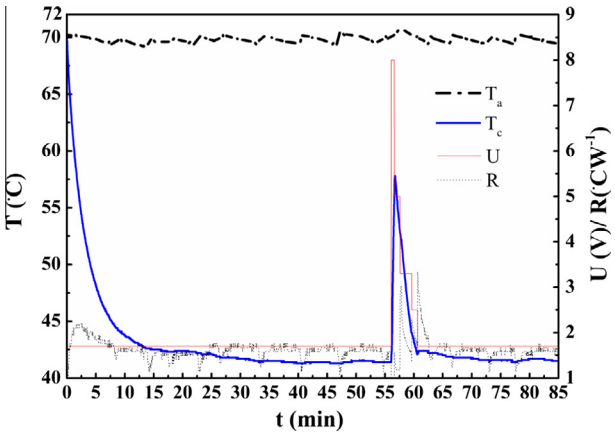

Fig. 9. Transient cold-end temperature (T_c) profiles of MTEM when cooling load experienced one step change and applied voltage experienced fifth step changes.

then increases to 65.7 °C. Then the applied voltage returns to 1.7 V, T_c decreases to the stable temperature, the overshoot sustains 15 min. Fig. 9 shows that when T_c firstly reaches stable at 41.4 °C, the applied voltage then starts step-changes and heater starts pulse-change, T_c rapidly increases to 57.8 °C and rapidly decrease to 42.2 °C. When the applied voltage returns to 1.7 V, T_c decreases to the stable temperature, the overshoot sustains 9.5 min. Comparing Fig. 8 with Fig. 9, the step-changes voltage reduces the hold time of overshoot.

Comparing Fig. 8 with Fig. 5, the temperature of numerical simulation profiles well captured general trends as shown in the experiment tests. But the pulse supercooling effect is unconspicuous in the experiment tests. Comparing Fig. 9 with Fig. 6, it is also found that the cold-end temperature does not experience the underdamped oscillation in the experiment test, and the cold temperatures in the experiment tests are larger than the cold temperatures in the numerical tests. Two reasons can be described the degradation phenomena in performance. Firstly, the thermocouple is placed in the heater which thermal capacity of heater results in the small decrease of the cold-end temperature and the sluggish response, and the cold temperature in the test is an indirect measurement value for the inevitable measurement error. On the other hand, the interface resistances result in the increase of

the cold-end temperature [15]. Furthermore, the t_p is equal to 30 s in experiment which is larger than the numerical value. This is because that the heater turning on and off and the step change voltage are manually controlled, so the t_p is set for 30 s for convenient operation. Therefore, the cold-end temperatures obtained in experiment tests are higher than those in simulation tests and the time scales in the results are different.

5. Conclusion

In summary, this study explores the scaling effect and transient supercooling effect of MTEM. It also develops a computation model for MTEM. The step-changes voltage for MTEM cooling pulse laser is investigated here. The profiles of the cold-end temperatures of MTEM when the applied voltage experiences step-change and pulse change are obtained from both numerical simulation and experiment tests, respectively. The analysis shows that the step-change voltage can be very effective to reduce the overshoot and hold time of overshoot. The efficient utilization of step-change voltage for pulse cooling load maybe produces a stable temperature for pulse laser. The numerical results agree well with the datasheet of MTEM and experimental data. An interesting phenomenon is also found that the voltage for achieving the maximum cooling capacity experiences step decrease with the increase of thermal resistance of hot-end heat exchanger. A fitting equation was developed to simulate the response of cold-end temperature. The fitting equation can also be applicable for the design and optimization of a temperature controller as well as proper thermal management for a laser module cooled by TEC. The numerical model can be applied to the performance prediction and optimization of miniature thermoelectric cooler. The simulation results can be used as feasibility and effectiveness reference by employing step-change voltage into MTEM for pulse laser cooling.

Acknowledgements

This work is supported by the National Natural Science Fund of China (Grant Nos. 51376068 and 51246005) and Research Fund for the Doctoral Program of Higher Education of China (Grant No. 20120142110045).

References

[1] Chang YJ, Chen YM, Lee CA, Wang YH, Chen YC, Wang CH. Improving temperature control of laser module using fuzzy logic theory. In: Semiconductor thermal measurement and management symposium, 2004. Twentieth Annual IEEE. 2004; p. 198–204.
[2] Phelan PE, Chiriac VA, Lee TYT. Current and future miniature refrigeration cooling technologies for high power microelectronics. Compo Pack Technol IEEE Trans 2002;25(3):356–65.
[3] Riffat SB, Ma XL. Thermoelectrics: a review of present and potential applications. Appl Therm Eng 2003;23(8):913–35.
[4] Semenyuk V. Miniature thermoelectric modules with increased cooling power. edito. Thermoelectrics, 2006. ICT '06. In: 25th International conference on; 2006. P. 322–6.
[5] Labudovic M, Jin L. Modeling of TE cooling of pump lasers. Comp Pack Technol IEEE Trans 2004;27(4):724–30.
[6] Jong-Jin L, Hyun-Seo K, Jai SK. Prediction of TEC power consumption for cooled laser diode module. edito. Lasers and Electro-Optics Society, 2004. LEOS 2004. In: The 17th annual meeting of the IEEE, vol. 2, 2004. p. 657–8.
[7] Zhiyong Z, Pu Z, Xiaoning L, Lingling X, Hui L, Zhiqiang N, Zhenfu W, Xingsheng L. Thermal modeling and analysis of high power semiconductor laser arrays. edito. Electronic Packaging Technology and High Density Packaging (ICEPT-HDP), 2012. In: 13th International conference on; 2012. p. 560–6.
[8] Donghan W, Shuang D, Ting G, Yong P, Bo Z, Hui L, Yi Q. Thermal characteristic analysis of new structure in 850nm VCSEL. edito. Optoelectronics and Microelectronics (ICOM), 2012. In: International conference on; 2012. p. 64–7.
[9] Xiaoning L, Yanxin Z, Jingwei W, Lingling X, Pu Z, Zhiqiang N, et al. Influence of package structure on the performance of the single emitter diode laser. Comp Pack Manuf Technol IEEE Trans 2012;2(10):1592–9.
[10] Daoming X, Yonggang Z, Xiaohui M, Yang L, Zibin Y, Li X, Wei Z, Qingxue S, Zhimin Z. Study on heat sink and solder of C-Mount packaged semiconductor laser. edito. Optoelectronics and Microelectronics (ICOM), 2012. In: International conference on; 2012. p. 68–72.
[11] Long R, Liu W, Xing F, Wang H. Numerical simulation of thermal behavior during laser metal deposition shaping. Trans Nonferrou Met Soc China 2008;18(3):691–9.
[12] Liu X, Hu MH, Caneau CG, Bhat R, Chung-en Z. Thermal management strategies for high power semiconductor pump lasers. Comp Pack Technol IEEE Trans 2006;29(2):268–76.
[13] Wang H, Yu Y. Dynamic modeling of PID temperature controller in a tunable laser module and wavelength transients of the controlled laser. Quantum Electr IEEE J 2012;48(11):1424–31.
[14] Novak V, Podobnik B, Možina J, Petkovšek R. Analysis of the thermal management system for a pump laser. Appl Therm Eng 2013;57(1–2):99–106.
[15] Shen LM, Xiao F, Chen HX, Wang SW. Numerical and experimental analysis of transient supercooling effect of voltage pulse on thermoelectric element. Int J Refrig 2012;35(4):1156–65.
[16] Tan FL, Fok SC. Methodology on sizing and selecting thermoelectric cooler from different manufacturers in cooling system design. Energy Convers Manage 2008;49(6):1715–23.
[17] Marlow Industries. The datasheet of SP5083. <http://www.marlow.com/media/-marlow/product/downloads/sp5083-03ac/SP5083.pdf>. 2013.11.19.
[18] Da Silva LW, Kaviany M. Micro-thermoelectric cooler: interfacial effects on thermal and electrical transport. Int J Heat Mass Trans 2004;47(10–11):2417–35.
[19] Xuan XC. Investigation of thermal contact effect on thermoelectric coolers. Energy Convers Manage 2003;44(3):399–410.
[20] Cheng C, Huang S, Cheng T. A three-dimensional theoretical model for predicting transient thermal behavior of thermoelectric coolers. Int J Heat Mass Trans 2010;53(9–10):2001–11.
[21] Lesage FJ, Pagé-Potvin N. Experimental analysis of peak power output of a thermoelectric liquid-to-liquid generator under an increasing electrical load resistance. Energy Convers Manage 2013;66:98–105.
[22] Hodes M. On one-dimensional analysis of thermoelectric modules (TEMs). Trans Comp Pack Technol 2005;28(2):218–29.
[23] Chen MA, Jeffrey Snyder G. Analytical and numerical parameter extraction for compact modeling of thermoelectric coolers. Int J Heat Mass Trans 2013:689–99.
[24] Ahiska R, Ahiska K. New method for investigation of parameters of real thermoelectric modules. Energy Convers Manage 2010;51:338–45.
[25] Chein R, Chen Y. Performances of thermoelectric cooler integrated with microchannel heat sinks. Int J Refrig 2005;28(6):828–39.
[26] Oshman CJ, Shi B, Li C, Yang RG, Lee YC, Bright VM. Fabrication and testing of a flat polymer micro heat pipe. edito. Solid-State Sensors. In: Actuators and microsystems conference, 2009. TRANSDUCERS 2009, 2009. p. 1999–2002.
[27] Liu X, Han T, Dong T, Wang C. A novel flat micro heat pipe with fiber wick. edito. Laser Physics and Laser Technologies (RCSLPLT) and 2010. In: Academic symposium on optoelectronics technology (ASOT), 2010 10th Russian-Chinese symposium on; 2010. p. 307–10.
[28] Yang RG, Chen G, Kumar AR, Snyder GJ, Fleurial JP. Transient cooling of thermoelectric coolers and its applications for microdevices. Energy Convers Manage 2005;46(9–10):1407–21.